Phytoplankton class-specific primary production in the world's oceans: Seasonal and interannual variability from satellite observations

Julia Uitz,[1] Hervé Claustre,[2] Bernard Gentili,[2] and Dariusz Stramski[1]

[1]   We apply an innovative approach to time series data of surface chlorophyll from satellite observations with SeaWiFS (Sea-viewing Wide Field-of-view Sensor) to estimate the primary production associated with three major phytoplankton classes (micro-, nano-, and picophytoplankton) within the world's oceans. Statistical relationships, determined from an extensive in situ database of phytoplankton pigments, are used to infer class-specific vertical profiles of chlorophyll a concentration from satellite-derived surface chlorophyll a. This information is combined with a primary production model and class-specific photophysiological parameters to compute global seasonal fields of class-specific primary production over a 10-year period from January 1998 through December 2007. Microphytoplankton (mostly diatoms) appear as a major contributor to total primary production in coastal upwelling systems (70%) and temperate and subpolar regions (50%) during the spring-summer season. The contribution of picophytoplankton (e.g., prokaryotes) reaches maximum values (45%) in subtropical oligotrophic gyres. Nanophytoplankton (e.g., prymnesiophytes) provide a ubiquitous, substantial contribution (30–60%). Annual global estimates of class-specific primary production amount to 15 Gt C yr^{-1} (32% of total), 20 Gt C yr^{-1} (44%) and 11 Gt C yr^{-1} (24%) for micro-, nano-, and picophytoplankton, respectively. The analysis of interannual variations revealed large anomalies in class-specific primary production as compared to the 10-year mean cycle in both the productive North Atlantic basin and the more stable equatorial Pacific upwelling. Microphytoplankton show the largest range of variability of the three phytoplankton classes on seasonal and interannual time scales. Our results contribute to an understanding and quantification of carbon cycle in the ocean.

1.   Introduction

[2]   Our understanding of oceanic biogeochemical cycles has benefited greatly from the recent advent of ocean color remote sensing. In particular, estimating marine primary production at the global scale represents one of the main applications of ocean color [e.g., *McClain*, 2009]. Such estimates rely on primary production models, which vary in formulation and complexity, but are largely based on the same theoretical background [*Bidigare et al.*, 1992; *Behrenfeld and Falkowski*, 1997a]. Typically, primary pro-

duction models require, as input parameters, the photosynthetically available radiation (PAR), an estimate of phytoplankton biomass (the concentration of chlorophyll a, Chl, or phytoplankton carbon), and a yield function that describes the phytoplankton photophysiological response to PAR. Combined with satellite-derived data of surface Chl (Chl_{surf}), primary production models enabled major achievements, including the quantification of global primary production [e.g., *Longhurst et al.*, 1995; *Antoine et al.*, 1996; *Behrenfeld and Falkowski*, 1997b; *Westberry et al.*, 2008] and the study of primary production variability on different spatiotemporal scales [e.g., *Bosc et al.*, 2004; *Behrenfeld et al.*, 2006]. Such applications have, however, focused so far only on the production associated with the entire phytoplankton assemblage, which does not resolve the effects of community composition on biogeochemical fluxes.

[3]   The taxonomic and size structure of phytoplankton communities influence many biogeochemical processes,

---

[1]Marine Physical Laboratory, Scripps Institution of Oceanography, University of California, San Diego, La Jolla, California, USA.
[2]UMR 7093, Laboratoire d'Océanographie de Villefranche, UPMC Université Paris 6, CNRS, Villefranche-sur-mer, France.

especially by regulating the photosynthetic efficiency of carbon fixation, the transfer of organic matter to higher trophic levels, and its export to the deep ocean through sinking [*Margalef*, 1965; *Kiørboe*, 1993; *Guidi et al.*, 2010]. For example, microphytoplankton (primarily diatoms) are considered to be responsible for new (i.e., nitrate-based) primary production and for contributing substantially to carbon export [*Eppley and Peterson*, 1979; *Michaels and Silver*, 1988; *Goldman*, 1993]. Thus, it has been recognized that accounting for phytoplankton community structure is of crucial importance to improve our understanding and modeling of oceanic biogeochemical cycles [*Aumont et al.*, 2003; *Le Quéré et al.*, 2005; *Hood et al.*, 2006].

[4] The development of algorithms for discriminating distinct groups of phytoplankton (species, taxa, or size classes) from ocean color remote sensing has become an area of active research [e.g., *Sathyendranath et al.*, 2004; *Alvain et al.*, 2005; *Ciotti and Bricaud*, 2006; *Uitz et al.*, 2006; *Hirata et al.*, 2008]. Although important and valuable, information retrieved from these algorithms does not allow a direct quantification of the impact of each phytoplankton group on the biological pump, and hence is limited for biogeochemical interpretation. The next desired advancement in research is to estimate the primary production associated with distinct groups forming the entire primary producer community. Only a few recent studies have focused on group-specific primary production modeling and were dedicated to regional applications [*Claustre et al.*, 2005; *Kameda and Ishizaka*, 2005; *Hirata et al.*, 2010].

[5] Estimating phytoplankton group-specific primary production may be done by combining ocean color-based primary production modeling with algorithms for detecting phytoplankton groups. In order to implement such an approach, two requirements need to be fulfilled. First, primary production models apply to Chl within the entire water column, rather than just the surface layer "seen" by remote sensing. Hence, vertical profiles of Chl specific to each group under consideration are required. Second, one needs to identify group-specific photophysiological properties. The algal photophysiological response is recognized to be dependent on the taxonomic composition and size structure [*Claustre et al.*, 1997; *Bouman et al.*, 2005; *Cermeño et al.*, 2005; *Uitz et al.*, 2008], so that using a single set of photophysiological properties regardless of the phytoplankton group would be inappropriate.

[6] *Uitz et al.* [2006] developed an approach for estimating the contributions of three pigment-based size classes (micro-, nano-, and picophytoplankton) to depth-resolved Chl using Chl$_{surf}$ as input information. This approach can be combined with the class-specific photophysiological properties from *Uitz et al.* [2008], and used as input to a primary production model to estimate the primary production associated with each phytoplankton size class.

[7] In this study, we apply the phytoplankton class-specific approach to the 10-year, global time series of SeaWiFS (Sea-viewing Wide Field-of-view Sensor) ocean color measurements to assess the contribution of the three phytoplankton classes to primary production within the world's open oceans. In addition to providing first satellite-based global estimates of class-specific primary production, this analysis enables the identification of seasonal and interannual patterns in the relative contribution of the different phytoplankton classes to total primary production.

2. Data and Methods

2.1. Primary Production Modeling

[8] The primary production model used in this study is the bio-optical model of *Morel* [1991]. The model relies on equation (1), which describes the mass of organic carbon photosynthetically fixed per unit water volume and time in terms of primary production rate (g C m^{-3} s^{-1}) occurring locally at a depth z and time instant t:

$$P(z,t,\lambda) = 12\ \mathrm{Chl}(z,t)\ a*(z,t,\lambda)\mathrm{PAR}(z,t,\lambda)\Phi_c(z,t,\lambda) \quad (1)$$

where Chl is in mg m^{-3}, $a*$ is the chlorophyll-specific absorption coefficient in units of m^2 (mg Chl)$^{-1}$, PAR is in mol quanta m^{-2} s^{-1}, and Φ_c is the irradiance-dependent quantum yield of carbon fixation in mol C (mol quanta)$^{-1}$. This model accounts for two main processes of photosynthesis, the absorption of radiant energy by algal pigments and its subsequent transformation into photosynthetic assimilate [*Antoine and Morel*, 1996]. The factor 12 enables the conversion of moles into grams of carbon. The integration of equation (1) with respect to λ, t, and z yields the desired quantity of daily primary production integrated vertically over the productive layer (P, g C m^{-2} d^{-1}). The depth of this layer is defined as 1.5 times the euphotic depth, Z_{eu}, where Z_{eu} is at the 1% level of surface PAR.

[9] We apply this model at the phytoplankton class-specific level in order to compute the primary production associated with micro- (P_{micro}), nano- (P_{nano}), and picophytoplankton (P_{pico}). The total primary production (P_{tot}), attributed to the whole algal biomass, is defined as the sum of the contributions of each class. The model requires the following inputs: the satellite-derived Chl$_{surf}$ and surface PAR, and the phytoplankton class-specific vertical profiles of Chl and photophysiological properties. The procedure used to derive these input variables is described in the following sections.

2.2. SeaWiFS Data

[10] We used monthly Level-3 GAC (Global Area Coverage) SeaWiFS data of Chl$_{surf}$ and surface PAR for the period from January 1998 through December 2007. Data were downloaded from the NASA Ocean Color website (http://oceancolor.gsfc.nasa.gov/). In order to keep the computing time at a reasonable level, the spatial resolution of images (1/12° × 1/12° at equator) has been reduced by binning the original pixels to form macro-pixels of resolution 1° × 1°. The spatial (1° × 1°) and temporal (one month) resolution of the input SeaWiFs images and computed primary production maps allow addressing global and basin-scale, as well as seasonal and interannual, patterns.

[11] As described in previous work [*Uitz et al.*, 2006, 2008], the phytoplankton class-specific approach was established using data sets collected in open ocean case-1
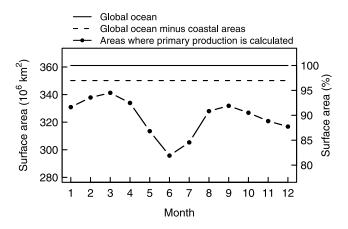
Figure 1. Monthly mean distribution of surface areas for (i) the global ocean, (ii) the global ocean excluding coastal areas with depths <200 m, large lakes, and inland seas, and (iii) the ocean areas accounted for in the present analysis (i.e., pixels for which a satellite-derived Chl_{surf} value was available). The left axis shows the surface area in absolute values (10^6 km^2), and the right axis shows the percent surface area relative to the surface area of the global ocean (%).

waters exclusively, and is thus applicable only to such environments. Therefore, pixels from coastal areas (i.e., bathymetry <200 m), large lakes, and inland seas were disregarded in this analysis. This represents 3% of the surface area of the global ocean (Figure 1). In addition, some areas are inaccessible to satellite observations due to cloud cover, low sun angle, sea ice, and lack of daylight. This is particularly true for high latitude (>50°) regions during winter months. As a result, the present analysis accounts for 82–95% of the surface area of the global ocean with maximum data coverage in spring and minimum in winter of each hemisphere.

2.3. Phytoplankton Class-Specific Chlorophyll

[12] Using an extensive pigment database obtained from high performance liquid chromatography (HPLC) analyses of water samples from a variety of oceanic regions, *Uitz et al.* [2006] proposed a method for deriving Chl vertical profiles associated with three pigment-based size classes (micro-, nano-, and picophytoplankton) from Chl_{surf}. Seven diagnostic pigments were selected as biomarkers of specific taxa. These taxa were then assigned to one of the three size classes (Table 1 and *Vidussi et al.* [2001, Table 1]). Some

limitations of this approach have been recognized at local and regional scales [*Vidussi et al.*, 2001; *Uitz et al.*, 2006]. For example, certain diagnostic pigments may be shared by various phytoplankton taxonomic groups, and some groups may have a wide range of cell size. Nevertheless, this approach has proven to be robust for large and global scale applications [*Uitz et al.*, 2006; *Ras et al.*, 2008] as it is indeed the case that microphytoplankton primarily include diatoms, nanophytoplankton prymnesiophytes, and picophytoplankton prokaryotic species. This approach thus provides valuable information pertaining to the taxonomic composition and size structure of phytoplankton communities [*Bricaud et al.*, 2004; *Uitz et al.*, 2009].

[13] Phytoplankton class-specific Chl vertical profiles were inferred, on a pixel-by-pixel basis, from SeaWiFS-derived Chl_{surf} data as detailed by *Uitz et al.* [2006]. In brief, the method requires determining whether the water column associated with each pixel is stratified or mixed. For this purpose, Z_{eu} was computed from Chl_{surf} (using *Uitz et al.* [2006, equation 8] and *Morel and Maritorena* [2001, equation 6]) and compared to the mixed layer depth (Z_m) extracted from the monthly climatology of *de Boyer Montégut et al.* [2004]. For stratified waters, Chl_{surf} was used to produce dimensionless (with respect to depth and biomass) profiles of class-specific Chl, which were converted to physical units by multiplying depths by Z_{eu}, and by multiplying dimensionless "concentrations" by the mean total (i.e., micro- + nano- + pico-) Chl within the euphotic layer. In the case of mixed layer conditions, the proportion of each phytoplankton class at the surface was derived from, and multiplied by, Chl_{surf}. This surface data product was extrapolated throughout the water column to generate uniform vertical profiles.

2.4. Phytoplankton Class-Specific Photophysiological Properties

[14] We use the vertical profiles of class-specific photophysiological properties that were proposed by *Uitz et al.* [2008]. They investigated relationships between phytoplankton photophysiology and community composition. This was done by analyzing a large database comprising HPLC-determined pigment concentrations, spectra of phytoplankton absorption coefficient, and photosynthesis-irradiance curve parameters, collected in various open ocean waters. An empirical model was proposed, which describes the dependence of algal photophysiological response on the community composition and irradiance within the water column, essentially reflecting photoacclimation. The appli-

Table 1. Diagnostic Pigments of Phytoplankton and Their Taxonomic and Size Class Association

Diagnostic Pigment	Taxonomic Association	Typical Cell Size	Phytoplankton Class
Fucoxanthin Peridinin	Diatoms Dinoflagellates	>20 μm	Microphytoplankton
19′-Hexfucoxanthin 19′-Butfucoxanthin Alloxanthin	Prymnesiophytes Pelagophytes Cryptophytes	2–20 μm	Nanophytoplankton
Zeaxanthin Total chlorophyll b (=chlorophyll b + divinyl-chlorophyll b)	Cyanobacteria, Prochlorophytes Chlorophytes, Prochlorophytes	<2 μm	Picophytoplankton

cation of the model to the in situ data set enabled the identification of depth-dependent photophysiological properties for each of the three pigment-based size classes.

[15] Although the database supporting the study of Uitz et al. [2008] was comprehensive in terms of covering differing trophic regimes, it consists of data collected only in tropical, subtropical, and temperate oceanic waters. Nevertheless, previous applications yielded reasonable estimates of class-specific primary production in two contrasted regions not included in the database, the Benguela upwelling system [Silió-Calzada et al., 2008] and the Kerguelen Island region in the Southern Ocean [Uitz et al., 2009]. Therefore, before an expanded database of relationships between the community composition and photophysiological parameters becomes available, the use of the Uitz et al. [2008] analysis appears reasonable for the world's open oceans with due caution.

[16] Additional information about the primary production model and the photophysiological properties can be found in Text S1.[1]

2.5. Climatology Calculations

[17] Global climatological seasonal maps of total and class-specific primary production were produced by averaging monthly values of each season over the 10-year SeaWiFS time series on a pixel-by-pixel basis. Months were grouped into seasons as follows: December–February for boreal winter/austral summer; March–May for boreal spring/austral fall; June–August for boreal summer/austral winter; September–November for boreal fall/austral spring. The global seasonal climatology is also presented as zonal median (less sensitive to outliers than the mean), in order to illustrate the variations in total and class-specific primary production as a function of latitude and season.

3. Results and Discussion

3.1. Climatology of Total and Class-Specific Primary Production

[18] In this section, we first briefly describe the spatio-seasonal distribution of total primary production, and then focus on the role of each phytoplankton class in determining this distribution.

3.1.1. Overview of the Distribution

[19] Figures 2 and 3 show the maps of total primary production, P_{tot}, obtained for the December–February and June–August seasons, respectively. These maps reveal typical regional and basin-scale patterns. Temperate and subpolar latitudes within each hemisphere exhibit high P_{tot} values in summer, most notably in the North Atlantic (>1 g C m^{-2} d^{-1}). These latitudes also show strong seasonality in P_{tot} (Figure 4a). At high latitudes $>50°$N and $>40°$S, the total primary production gradually increases from winter to summer, and then decreases from summer to winter, reflecting seasonal changes in light and nutrient availability. The seasonal pattern is reduced in the southern

hemisphere as compared to the northern one, due to the lower magnitude of spring-summer phytoplankton blooms. In contrast, oligotrophic subtropical gyres are typically associated with low P_{tot} values (0.3 g C m^{-2} d^{-1}) and show weak seasonality. The highest primary production rates are found in near-coastal regions, such as the major upwelling systems off western African and American coasts, where cold nutrient-rich waters rise to the surface and fuel phytoplankton growth (P_{tot} occasionally reaches 3 g C m^{-2} d^{-1}).
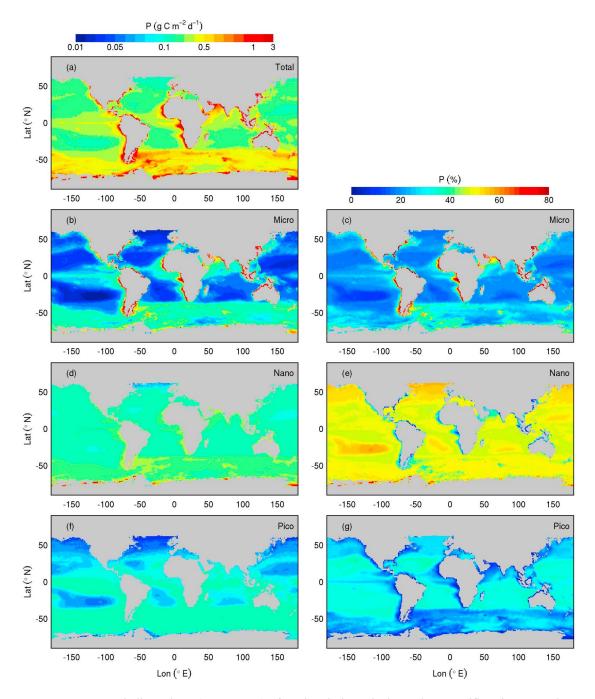
[20] The distribution of microphytoplankton production mostly mimics that of total primary production (Figures 2b–2c, 3b–3c, and 4b), which suggests that this class is responsible for most P_{tot} variations. Microphytoplankton appear as a major contributor to total primary production in temperate and subpolar latitudes in spring-summer, especially in the North Atlantic ($>50\%$) and in the Southern Ocean (30–50%). Their contribution reaches a maximum of about 70% in coastal upwelling systems year-round, with P_{micro} rates of up to 1 g C m^{-2} d^{-1}. It is also significant within the equatorial divergence (about 30% with P_{micro} of 0.1 g C m^{-2} d^{-1}), but is reduced drastically in subtropical gyres. The minimum P_{micro} rate (0.025 g C m^{-2} d^{-1} or 15% of P_{tot}) is found under extreme oligotrophic conditions encountered in the center of the South Pacific Subtropical Gyre in austral summer.

[21] Nanophytoplankton (Figures 2d–2e, 3d–3e, and 4c) appear ubiquitous and account consistently for a significant fraction of primary production, both in terms of absolute (0.07–1 g C m^{-2} d^{-1}) and relative contribution (30–60%). The highest P_{nano} values are observed at high latitudes, most notably in the Southern Ocean where they dominate seasonal blooms.

[22] Picophytoplankton production (Figures 2f–2g, 3f–3g, and 4d) shows consistently low values (<0.15 g C m^{-2} d^{-1}) regardless of the area, but nevertheless represents up to 40–45% of total production in oligotrophic subtropical waters. The relative contribution of picophytoplankton decreases to its minimum (15%) in the northernmost latitudes in summer, when P_{pico} is among its highest levels (0.1 g C m^{-2} d^{-1}).

[23] The coefficient of variation, defined as the ratio of the standard deviation to the mean value calculated over the entire time series, illustrates the temporal variability of class-specific primary production (Figure 5). Although calculated over the entire time series, the coefficients of variation are strongly driven by the seasonal cycle. The spatial distribution of the coefficient of variation follows the well-known trend of highly dynamic temperate and subpolar latitudes and significantly less variable equatorial and subtropical areas. These trends have been already reported for global estimates of total primary production [Behrenfeld et al., 2005; Lutz et al., 2007]. Microphytoplankton show maximum coefficients of variation poleward of 40° latitude in the North Atlantic and Pacific, as well as in the Atlantic and Indian sectors of the Southern Ocean (Figure 5a). P_{micro} also exhibits some degree of variability along the equator and within fairly stable subtropical gyres. Nano- and pico-phytoplankton show maximum coefficients of variation in the Southern Ocean and in the temperate and subpolar North

---

[1]Auxiliary materials are available in the HTML. doi:10.1029/2009GB003680.

Figure 2. Seasonal climatology (1998–2007) of total and phytoplankton class-specific primary production for the December–February period (boreal winter/austral summer). The left-hand panels show the primary production in absolute units of g C m^{-2} d^{-1}, and the right-hand panels show the percent contribution of class-specific production to total primary production.

Atlantic, and minimum values within the intertropical band (Figures 5b–5c). Microphytoplankton clearly exhibit the largest temporal dynamics of the three phytoplankton classes. For example, at latitude 50°N in the North Atlantic, maximum coefficients are 1.2, 0.5 and 0.4 for P$_{micro}$, P$_{nano}$, and P$_{pico}$, respectively.

3.1.2. Relation to Environmental Conditions

[24] The above-described patterns reflect the generally acknowledged distribution of phytoplankton groups in the world's oceans. Microphytoplankton, primarily diatoms, are known to develop preferentially in dynamic environments where light and fresh nutrients are available [*Malone*, 1980; *Goldman*, 1993]. This is especially the case in coastal
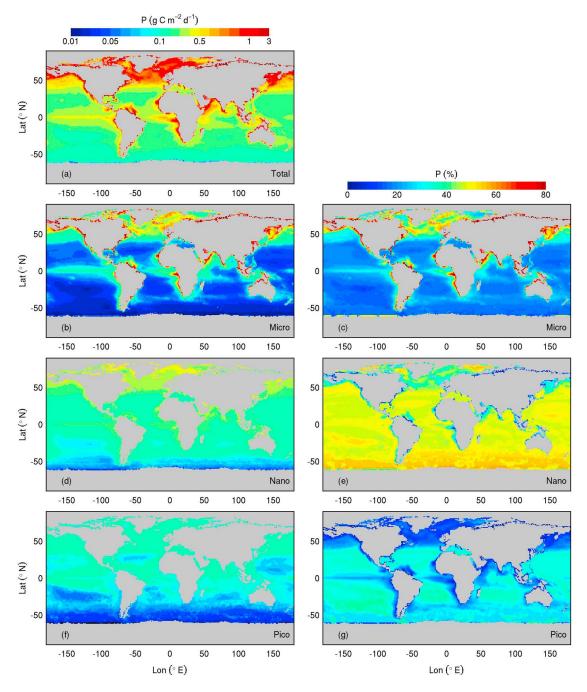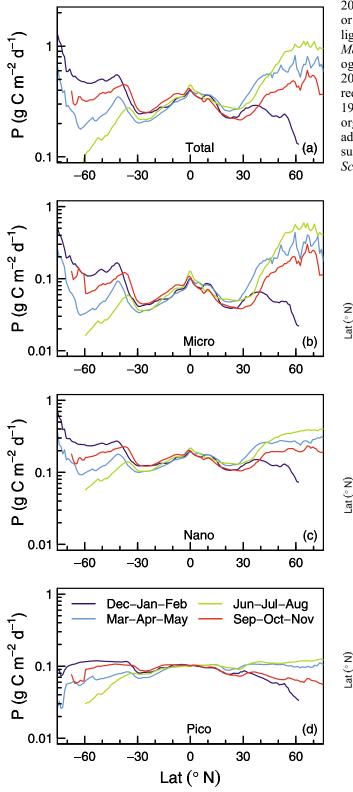
Figure 3. As Figure 2 but for the June–August period (boreal summer/austral winter).
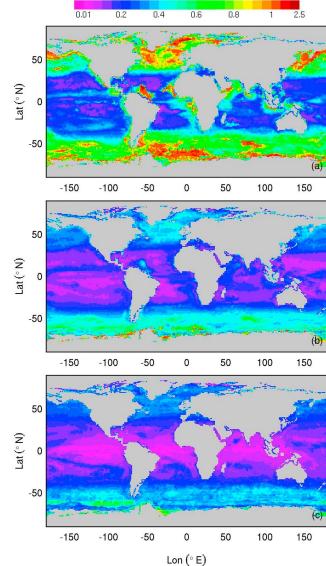
upwelling systems where nutrients are supplied with high frequency pulses, and in high latitudes areas (in spring or summer) where nutrients are replenished through vigorous winter mixing. Diatoms rapidly benefit from these growth-favorable conditions and outcompete other phytoplankton groups to form prominent blooms [*Falkowski et al.*, 2004]. In our photophysiological model, microphytoplankton are indeed more efficient in photosynthesis than other groups [*Claustre et al.*, 1997; *Cermeño et al.*, 2005; *Claustre et al.*, 2005; *Uitz et al.*, 2008].

[25] The reduced seasonality observed in the southern hemisphere is associated with a dominance of nanophytoplankton during the growth season. This feature primarily results from the high Chl biomass associated with nanophytoplankton in moderate bloom conditions and mixed southern waters [*Uitz et al.*, 2006]. This effect is further accentuated by the class-specific photoacclimation properties. The nanophytoplankton class is characterized by a large coefficient of light utilization (i.e., the slope of the so-called photosynthesis versus irradiance curve), which enables

efficient growth in light-limited conditions [*Uitz et al.*, 2008]. The environmental factors, including iron limitation or strong vertical mixing with subsequent relatively low light regime, explain these patterns [*Mitchell et al.*, 1991; *Martin et al.*, 1991; *Boyd*, 2002]. Large diatoms are recognized to be severely limited by iron availability [*Boyd*, 2002] and, although adapted to dynamic environments, require a period of stability to actually thrive [*Cailliau et al.*, 1997; *Goffart et al.*, 2000]. In contrast, certain nanoplankton organisms, like *Phaeocystis spp.*, are known to be well adapted to turbulent light-limited conditions and form large summer blooms at high southern latitudes [*Boyd*, 2002; *Schoemann et al.*, 2005].

Figure 4. Zonal median of seasonal climatology (1998–2007) of total and phytoplankton class-specific primary production. The color coding for different seasons is shown in the bottom panel.

Figure 5. Geographic distribution of the coefficient of variation (i.e., standard deviation normalized to the mean) of primary production associated with (a) micro-, (b) nano-, and (c) picophytoplankton for the 1998–2007 time period.

Table 2. Annual Total and Class-Specific Primary Production for the Global Ocean and for Various Oceanic Regions Excluding Coastal Areas (i.e., Bathymetry < 200 m), Large Lakes, and Inland Seas[a]

	P_{tot} (Gt C yr^{-1})	P_{micro} (Gt C yr^{-1})	P_{nano} (Gt C yr^{-1})	P_{pico} (Gt C yr^{-1})	P_{tot} Region/Global (%)	P_{micro}/P_{tot} (%)	P_{nano}/P_{tot} (%)	P_{pico}/P_{tot} (%)	Surface Area (%)
Global	45.6	14.8	20.0	10.8	100	32	44	24	100
Atlantic	12.2	4.6	5.0	2.5	27	38	41	21	22
Atlantic N	7.2	2.9	2.9	1.4	16	41	40	20	12
Atlantic S	5.0	1.7	2.2	1.1	11	35	43	22	10
Pacific	20.0	5.9	9.0	5.1	44	30	45	25	45
Pacific N	10.9	3.5	4.8	2.6	24	32	44	24	23
Pacific S	9.1	2.4	4.2	2.5	20	26	46	28	22
Indian	9.0	2.9	4.0	2.1	20	32	44	24	18
Indian N	2.8	1.2	1.0	0.5	6	45	38	17	4
Indian S	6.2	1.6	2.9	1.7	14	26	47	27	14
Arctic	0.5	0.3	0.2	0.1	1	55	34	11	1
Southern	3.5	0.9	1.7	0.8	8	26	50	24	12
Mediterranean Sea	0.5	0.2	0.2	0.1	1	36	42	22	1
Tropical	21.1	6.7	9.2	5.3	46	32	43	25	44
Equatorial	10.7	3.5	4.6	2.6	24	33	43	24	20

[a]The global ocean was divided into six ocean basins: Atlantic, Pacific, Indian, Arctic, the Southern Ocean, and the Mediterranean Sea. The northern boundary of the Southern Ocean is at the latitude of 50°S and the southern boundary of the Arctic zone is at 70°N. In addition, data are shown for two latitudinal bands of the global ocean: the intertropical and equatorial bands. The intertropical band is delimited by the latitudes of 23°N and 23°S and the equatorial band by the latitudes 10°N and 10°S. The reference surface area of the global ocean is 353 10^6 km^2.

[26] Another asymmetry can be observed between the North Atlantic and the North Pacific Oceans. Microphytoplankton production shows a reduced contribution to production in the subarctic Pacific, especially in the eastern part of the basin (Figure 3c). This feature has been observed for both Chl biomass and primary production and is commonly attributed to diatoms growing under iron limitation [*Miller et al.*, 1991; *Harrison et al.*, 1999].

[27] Picophytoplankton, especially cyanobacteria and prochlorophytes, form the characteristic community within oligotrophic subtropical gyres, where environmental forcing is relatively stable with high surface PAR and limited supply of nutrients to the euphotic zone [e.g., *Longhurst*, 2007]. The small-sized cells have higher surface to volume ratio than larger cells, which provides a better nutrient uptake capacity and, generally, an advantage over larger cells in nutrient-limited conditions [*Raven*, 1998]. Field observations typically report the dominance of picophytoplankton in subtropical waters in terms of biomass or cellular abundance [*Chisholm*, 1992; *Partensky et al.*, 1999; *Dandonneau et al.*, 2004; *Ras et al.*, 2008]. Nevertheless, our results show that picophytoplankton play a substantial, but not dominant, role in primary production in these waters. This is consistent with observations of *Li* [1994] who reported a dominance in terms of cellular abundance, but lower carbon uptake rates, for small (pico-sized) cells compared to larger (nano-sized) cells, at several open ocean sites in the North Atlantic. Although picophytoplankton contribute 50–55% to total integrated Chl content [*Uitz et al.*, 2006], this class is characterized by relatively low photosynthetic efficiency

[*Uitz et al.*, 2008], which likely results from a slow nutrient-limited growth [*Falkowski et al.*, 1992; *Marañon et al.*, 2000]. This explains the somewhat reduced contribution of picophytoplankton to total primary production.

[28] Previous studies revealed high biomass contribution of 19′-hexanoyloxyfucoxanthin (Hex) and 19′-butanoyloxyfucoxanthin containing organisms in oligotrophic subtropical regions [*Claustre and Marty*, 1995; *Ras et al.*, 2008; *Aiken et al.*, 2009]. These observations support the substantial contribution of prymnesiophytes (nanophytoplankton class) in these waters. Prymnesiophytes are recognized as a ubiquitous group often associated with transition zones between different environmental conditions [*Ondrusek et al.*, 1991; *Claustre et al.*, 1994; *Jordan and Chamberlain*, 1997]. The present results clearly emphasize they are able to sustain growth in a large variety of environments, ranging from stratified oligotrophic waters to harsh wintertime subantarctic conditions. Based on a combination of genetic tools and the pigment-based approach of *Uitz et al.* [2006], *Liu et al.* [2009] related the persistent presence and pigment biomass dominance of prymnesiophytes to their extreme, rather unsuspected, biodiversity. The taxonomic and ecological diversity of prymnesiophytes, notably their mixotrophic character, likely explain the success of this group in the world's open oceans.

3.1.3. Annual Global and Regional Estimates

[29] The phytoplankton class-specific approach yields a value of 46 Gt C yr^{-1} for the annual total primary production within the world's oceans (Table 2). This falls within the range of previously published estimates (36.5–56 Gt C yr^{-1})

based on satellite ocean color algorithms [*Longhurst et al.*, 1995; *Antoine et al.*, 1996; *Westberry et al.*, 2008] and biogeochemical models [*Moore et al.*, 2002; *Aumont et al.*, 2003]. In addition to mathematical formulations and input photophysiological parameters, which are specific to each model, the differences between the estimates may arise from several factors: (i) the Chl and PAR input data (selected years and satellite); (ii) the inclusion/exclusion of coastal or case-2 waters; and (iii) the integration depth. For example, integrating primary production within the euphotic layer instead of the productive layer (i.e., the layer $0–1.5Z_{eu}$) would decrease our global estimate by 7%. Despite this, all estimates are constrained within a reasonable range, which lends confidence to our approach.

[30] A comparison of our climatological P_{tot} estimates with those of *Antoine et al.* [1996] provides a means of evaluating how the bio-optical model of *Morel* [1991] performs when run without phytoplankton class-specific information. *Antoine et al.* [1996] utilized the *Morel* [1991] model with satellite-derived vertical profiles of Chl as given by *Morel and Berthon* [1989] and the photophysiological parameters from *Morel et al.* [1996]. As in the present study, the ratio of photosynthetically active pigments to the sum of photosynthetically active and degraded pigments (i.e., Chl + pheopigments) was considered to equal 1. The Chl_{surf} data derived from the Coastal Zone Color Scanner (CZCS) were used as inputs and case-2 water pixels were excluded. The two model formulations, that is, with and without class-specific information, yield identical P_{tot} estimates for the global ocean.

[31] We also estimated the annual primary production integrated for six ocean basins (Atlantic, Pacific, Indian, Arctic, the Southern Ocean, and the Mediterranean Sea), as well as for the equatorial and intertropical latitudinal zones (Table 2). We compared our regional P_{tot} estimates with those of *Antoine et al.* [1996]. The contribution of the Atlantic, Pacific, and Indian basins to the global total primary production obtained from the two model formulations are in close agreement. However, we observe important differences when low and high latitude regions are considered separately. Our P_{tot} estimate is lower than that of *Antoine et al.* [1996] by about 15% and 20% for the equatorial and intertropical latitudinal zones, respectively. In contrast, our estimate is higher than that of *Antoine et al.* [1996] by 50% in the Arctic Ocean. Our phytoplankton class-specific approach yields lower primary production rates at low latitudes due to the relatively low photosynthetic efficiency of small (pico- and nano-) phytoplankton which dominate the algal biomass. In the Arctic Ocean, primary production is mainly associated with microphytoplankton which are more efficient in photosynthesis than smaller cells. In addition, the differences observed between the results of the two model formulations arise from the photosynthesis dependence on temperature in the *Antoine et al.* [1996] model, which causes an increase of primary production at low latitudes and a decrease at high latitudes.

[32] The global annual class-specific primary production amounts to 15 Gt C yr^{-1} (32% of the total), 20 Gt C yr^{-1} (44%), and 11 Gt C yr^{-1} (24%) for micro-, nano-, and picophytoplankton, respectively. Previous global estimates of primary production attributable to diatoms vary within a threefold range of 9–26 Gt C yr^{-1}, corresponding to 20–40% of total primary production [*Tréguer et al.*, 1995; *Moore et al.*, 2002; *Aumont et al.*, 2003]. *Falkowski and Raven* [1997] proposed a lower limit of 10% for global primary production associated with picophytoplankton. *Agawin et al.* [2000] assessed that picophytoplankton production amounts to 19 Gt C yr^{-1}, or 39% of total primary production. Despite the diversity in the approaches used to generate these global estimates (e.g., biogeochemical models including several phytoplankton groups, budgets of biogeochemical elements), our estimates are close to the mean of reported values.

[33] With regards to regional estimates of class-specific production, the contribution of P_{nano} varies within a quite restricted range from 34% in the Arctic to 50% in the Southern Ocean. The relative contributions of micro- and picophytoplankton show inverse regional distributions. Whereas the highest contribution of microphytoplankton is found in the Arctic (55%), the picophytoplankton contribution in that region is minimal (11%). In contrast, the lowest contribution of microphytoplankton is found in the South Pacific (26%), where the picophytoplankton contribution is maximum (28%). The contribution of microphytoplankton to total regional primary production reaches maximum values in the northern hemisphere basins with about 40% in the Atlantic and Indian Oceans, 55% in the Arctic, and 32% in the Pacific Ocean.

3.1.4. Microphytoplankton Production as a Biogeochemical Index

[34] Microphytoplankton, in particular diatoms, are generally recognized as a main contributor to new (nitrate-supported) primary production [*Goldman*, 1993]. Based on this postulate, *Claustre* [1994] proposed the pigment index F_p, as a measure of the relative contribution of microphytoplankton to the total phytoplankton biomass. Strong similarities between F_p and the *f*-ratio (i.e., the ratio of new to total primary production; [*Eppley and Peterson,* 1979]) were observed, so that F_p can be used as a proxy for the *f*-ratio. By extending the pigment approach of *Claustre* [1994], we propose the F_{prod} index defined as the relative contribution of microphytoplankton to the total primary production (i.e., the P_{micro}/P_{tot} ratio).

[35] The F_{prod} index is as high as 0.7–0.8 in coastal upwelling systems and 0.5–0.7 in the North Atlantic during the spring-summer bloom (Figures 2c and 3c). Minimum values (0.1–0.2) are found in oligotrophic subtropical gyres and intermediate values (0.3) within mesotrophic areas such as the equatorial divergence. These estimates are consistent with *f*-ratio values reported in the literature for various trophic situations. For instance, coastal upwellings are typically characterized by *f*-ratio >0.5 [*Eppley and Peterson*, 1979; *Kudela and Dugdale*, 2000], occasionally reaching 0.8 [*Eppley and Peterson*, 1979; *Dugdale and Wilkerson*, 1992]. *Bury et al.* [2001] measured values of 0.5 during a diatom bloom in the North Atlantic. In subtropical gyres, the *f*-ratio is usually in the range 0.05–0.15 [*Eppley and Peterson*, 1979; *Dugdale and Wilkerson*, 1992; *Laws et al.*, 2000].

[36] Similarities in the general distribution of the F_{prod} index and *f*-ratio support the view that, on large spatial and time scales, diatoms play a dominant role in new primary production, which is subsequently available for carbon export to the deep ocean. These results highlight the potential of microphytoplankton-specific production estimate as a useful biogeochemical indicator.

[37] In addition, a review of several studies indicates that the export flux of carbon out of the euphotic zone ranges within 10–16 Gt C yr^{-1}, which would represent 20–40% of the total primary production [*Tréguer et al.*, 2003]. These results are consistent with our global annual estimate of P_{micro} (15 Gt C yr^{-1}, or 32%). Our results are also in qualitative agreement with the global climatology of carbon export proposed by *Lutz et al.* [2007], showing maximum values at high northern latitudes, specifically in the North Atlantic, and in coastal upwelling systems.

3.2. Annual Cycle and Interannual Variability

[38] In this section we present the mean annual cycle and interannual variability of total and class-specific primary production for the global ocean and two different regions of particular interest, the equatorial Pacific upwelling and the temperate and subpolar North Atlantic. The equatorial Pacific region has received considerable attention due to its High Nutrient Low Chlorophyll (HNLC) nature and the fact that it is the most important oceanic source of CO_2 to the atmosphere [*Takahashi et al.*, 2009]. In contrast, the North Atlantic Ocean represents a large CO_2 sink [*Takahashi et al.*, 2009], and supports one of the largest open ocean phytoplankton blooms observable from space [e.g., *Yoder et al.*, 1993]. Here we examine the interannual variability by comparing the annual cycle of each year to the mean climatological (1998–2007) annual cycle. The percentage anomalies of total and class-specific primary production were calculated as a difference between each monthly value and the 10-year monthly mean, which was normalized to the 10-year monthly mean.

3.2.1. Global Ocean

[39] The mean annual cycle of total primary production shows two peaks of almost equal amplitude (about 0.4 g C m^{-2} d^{-1}) in June and December, associated with the occurrence of a spring-summer bloom in each hemisphere (Figures 6a and 7a). Total primary production is dominated by the contribution of nanophytoplankton (40–45%) all year long. The three phytoplankton classes exhibit two peaks in primary production. However, the maximum of P_{micro} is mostly associated with the northern hemisphere bloom (July), while the maxima of P_{nano} and P_{pico} are mostly associated with the southern hemisphere bloom (December–January).

[40] There is relatively little interannual variability in the annual cycle of total and class-specific primary production over the global ocean (Figure 7), which is not surprising given the large extent of the averaging area. For example, P_{tot} ranges between 0.35 g C d^{-1} (March 1998) and 0.41 g C d^{-1} (December 1998), and P_{tot} anomalies between −3% and 2%. Nevertheless, we observe a different degree of variability among the different phytoplankton classes, from micro- (anomalies between −6% and 5%), to
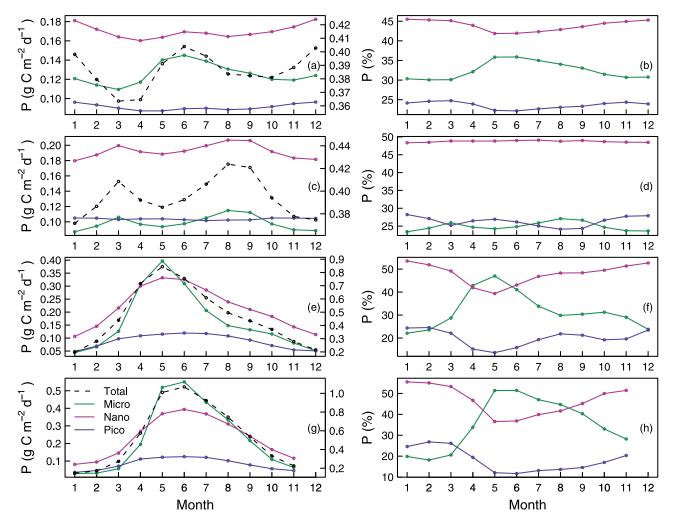
nano- (anomalies between −3% and 2%), and picophytoplankton (anomalies of ±1%). In contrast to the observations made on the global scale, the regional scale analysis reveals large year-to-year variations in total and class-specific primary production.

3.2.2. Equatorial Pacific Upwelling

[41] The equatorial Pacific upwelling system is characterized by the presence of a quasi-stationary upwelling driven by northeast and southeast trade winds. Upwelling of cool water through the shallow thermocline results in a large supply of nutrients to the surface layer, which supports higher Chl concentrations and primary production compared with surrounding waters [*Chavez and Barber*, 1987; *Chavez et al.*, 1996]. As seen in Figures 6c–6d, total primary production shows moderate values (≈0.4 g C m^{-2} d^{-1}) with a weak seasonal cycle. Two relatively low maxima are observed in March–April and August–September, which is likely related to weak changes in trade wind activity [*Yoder and Kennelly*, 2003]. Our climatological (1998–2007) mean is comparable to that reported by *Chavez et al.* [1990] (0.45 g C m^{-2} d^{-1}), but about twice lower than more recent estimates [*Chavez et al.*, 1996]. Although methodological issues have been raised to explain these discrepancies, some debate is still ongoing [*Pennington et al.*, 2006].

[42] Despite a constantly favorable light/nutrient regime, nitrate is never depleted and Chl biomass and primary production are relatively low considering the nutrient levels in the area [*Barber and Chavez*, 1991]. This HNLC character has been extensively discussed [*Chisholm and Morel*, 1991], and appears to be primarily due to iron limitation [*Barber and Chavez*, 1991; *Coale et al.*, 1996] and, to a lesser extent, to regulation by silicate [*Dugdale and Wilkerson*, 1998] and grazing [*Smetacek*, 1999]. These environmental conditions favor a phytoplankton community dominated by small cells [*Chavez et al.*, 1990, 1996; *Moon van der Staay et al.*, 2000], so that our microphytoplankton class actually refers to small (nano- sized) diatoms. Note that large diatoms have been observed on some occasions in the Pacific equatorial region and were associated with higher productivity [*Chavez et al.*, 1996]. Figures 6c–6d show that nanophytoplankton are the main contributor to total primary production throughout all year (>45%), while picophytoplankton and diatoms contribute the remaining portion (25–30% each). Based on previous observations [*Blanchot et al.*, 2001; *Dandonneau et al.*, 2004], our results may underestimate the contribution of picophytoplankton to primary production to the benefit of other groups. However, assuming that diatoms are responsible for new primary production, our estimate of the relative contribution of diatoms to total primary production (i.e., F_{prod} index) is consistent with previously reported *f*-ratio values of about 0.3 [*Chavez and Barber*, 1987; *Fiedler et al.*, 1991].

[43] As shown in Figure 8, total and class-specific primary production in the equatorial Pacific upwelling is subject to important year-to-year changes. This is primarily linked to variability in physical forcing in response to the periodic occurrence of El Niño and La Niña episodes [e.g., *Chavez et al.*, 1996]. The most remarkable perturbation appears related to the strong 1997–1999 El Niño/La Niña
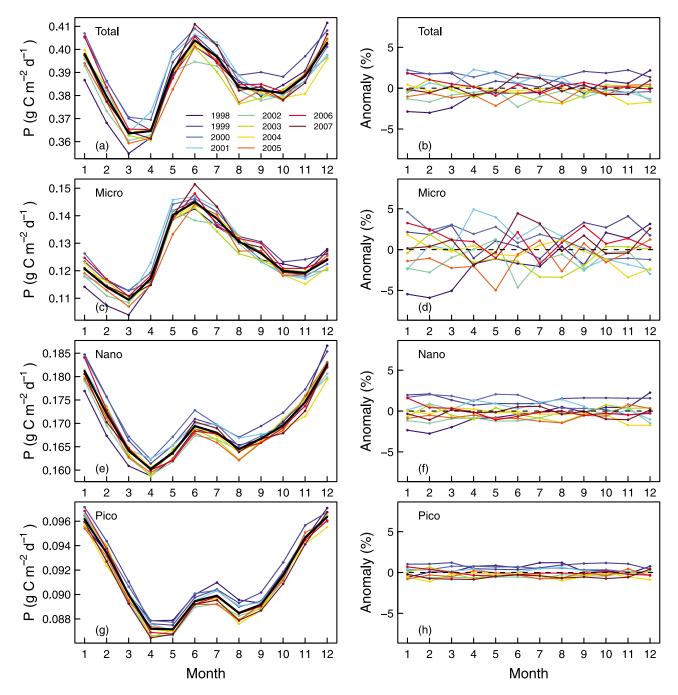
Figure 6. Climatological mean (1998–2007) annual cycle of total and phytoplankton class-specific primary production calculated over the (a–b) global ocean, (c–d) equatorial Pacific upwelling [5°N–5°S; 150°W–90°W], (e–f) temperate North Atlantic [40°N–50°N; 10°W–60°W], and (g–h) subpolar North Atlantic [50°N–70°N; 10°W–60°W]. Results are presented as absolute primary production rates (g C m^{-2} d^{-1}) for total and class-specific primary production (Figures 6a, 6c, 6e, and 6g), and as a fraction of total primary production (%) for class-specific primary production (Figures 6b, 6d, 6f, and 6h). Note the two different axes for absolute primary production rates (Figures 6a, 6c, 6e, and 6g): the left axis is for class-specific primary production rates and the right axis for total primary production rates.

event [*McPhaden*, 1999]. Total and diatom primary production shows high negative anomalies (−20% and −33%, respectively) in January 1998 due to the passage of El Niño. This event essentially causes a weakening (or a reversal) of the trade winds, which removes the driving force of the upwelling and deepens the thermocline. Surface waters become warm and nutrient-poor, typically leading to a decrease in Chl biomass and primary production. This perturbation is followed by a large increase in diatom production (+53%) in August 1998. This is associated with the subsequent development of a strong La Niña when the pattern is reversed and cold nutrient-rich waters are upwelled more strongly. Consistent with previous observations [*Chavez et al.*, 1990; *Strutton and Chavez*, 2000], diatoms appear to be the most responsive group to these changes with P$_{micro}$

anomalies ranging between −37% and 53%. The maximum range of variation was −21% to 13%, and −8% to 3% for nano- and picophytoplankton production, respectively.

[44] A second perturbation is observed in 2005–2006. Primary production shows a negative anomaly (−16% for diatoms) in April 2005, followed by a return to near-normal values by the end of 2005, and a raise to above-normal values in March 2006 (+24% for diatoms). This feature is related to the moderate 2005–2006 El Niño/La Niña event, whose fingerprint is greatly reduced as compared to the 1997–1999 phenomenon.

3.2.3. Temperate and Subpolar North Atlantic

[45] Temperate and subpolar latitudes are characterized by a well-known pattern with the occurrence of an intense spring-summer bloom [*Sverdrup*, 1953]. Deep winter mix-

Figure 7. Time series (1998–2007) of total and phytoplankton class-specific primary production for the global ocean. Results are presented as (a, c, e, and g) primary production rates and (b, d, f, and h) relative anomalies calculated as the difference between the primary production value for a given month and the climatological mean value for that month, normalized to the climatological monthly mean (1998–2007) value. The black line represents the climatological mean.

ing, driven by strong winds and associated heat loss from the surface ocean, replenishes nutrients and sets up the nutrient stock available to phytoplankton in spring [*Koeve*, 2001]. Phytoplankton growth is then limited by insufficient light exposure, and can only occur in spring when stratification maintains phytoplankton and nutrients within the sunlit layer of the ocean.

[46] At temperate latitudes (Figures 6e and 6f), the mean annual cycle of P_{tot} exhibits a prominent maximum in May (0.8 g C m^{-2} d^{-1}). This seasonal bloom is typically dominated by large diatoms (P_{micro} is 50% of P_{tot}) and nano-phytoplankton (40%). In mid-summer as stratification increases, nutrients become depleted, the grazer community develops, and the production of diatoms declines in favor of
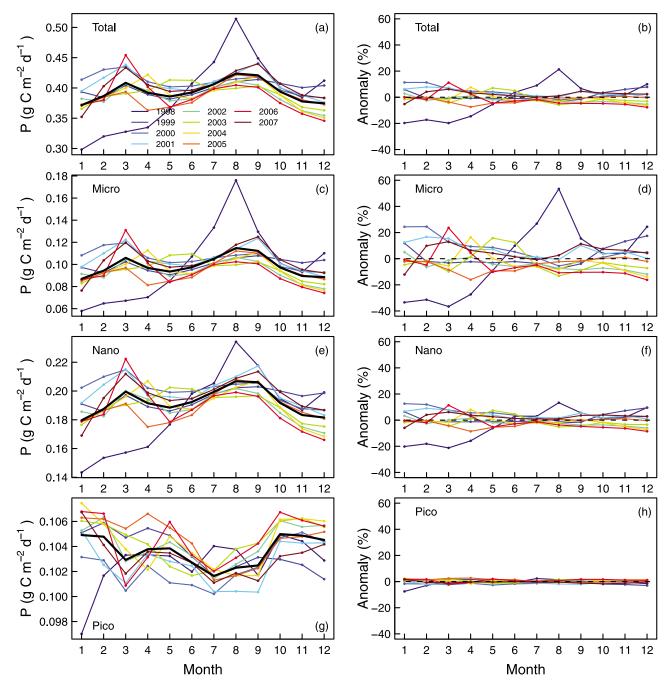
Figure 8. As Figure 7, but for the equatorial Pacific upwelling [5°N–5°S; 150°W–90°W].

nanophytoplankton [*Lochte et al.*, 1993], often coccolitho-phorids [*Holligan et al.*, 1993; *Iglesias-Rodriguez et al.*, 2002]. The contribution of nanophytoplankton to primary production remains substantial all year long (40–54%), while that of picophytoplankton ranges within 14–25%. A secondary production event (P_{tot} of 0.4 g C m^{-2} d^{-1}) may be observed in fall (September–October), mostly associated with a slight increase in the contribution of micro- and nanophytoplankton to primary production. At temperate latitudes, fall blooms often develop subsequently to nutri-cline shoaling driven by episodic mixing events [*Dickey et al.*, 2001; *Findlay et al.*, 2006].

[47] The mean annual cycle at subpolar latitudes shows several differences as compared to that in temperate areas (Figures 6g and 6h). The seasonal maximum of primary production is higher (P_{tot} > 1 g C m^{-2} d^{-1}) and associated with a larger contribution of diatoms (>50%). This maximum occurs one month later (in June) due to the delayed onset of stratification resulting from a reduced daylight period. Finally, the bloom period extends longer and does not display any fall event.
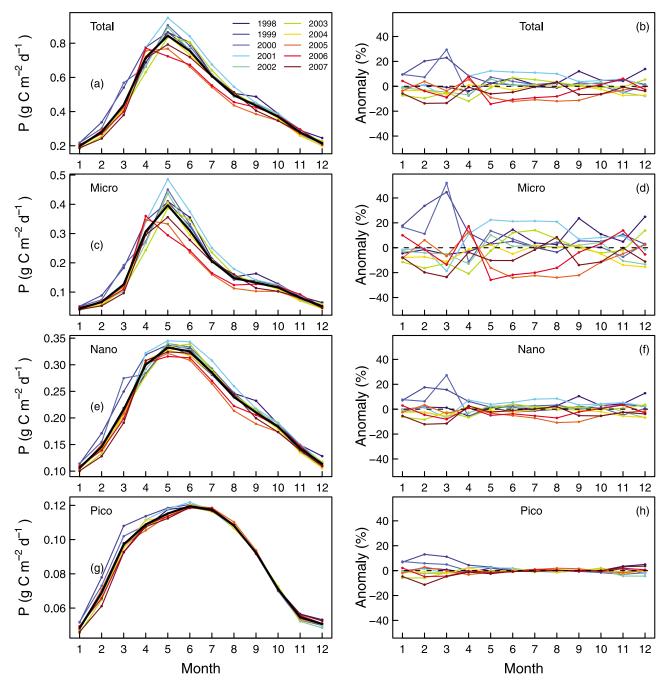
Figure 9. As Figure 7, but for the temperate North Atlantic [40°N–50°N; 10°W–60°W].

[48] In addition to this annual pattern, primary production exhibits large interannual variations related to changes in the timing and magnitude of the bloom, especially at temperate latitudes (Figure 9). For example, the 1999 annual cycle shows an early (February–March) increase in total primary production associated with larger contributions of small cells and microphytoplankton (P_{micro} anomaly of +45%) as compared to the 10-year mean. The 2001 annual cycle is characterized by an intense spring-summer bloom with an increase in diatom production (P_{micro} anomaly of +22%). The bloom period extends longer compared to the bloom

period of the mean annual cycle. Also, in 2001 no fall event is observed. In 2006, the bloom peaks early in April, then exhibits low values and further declines rapidly throughout summer. Again, nanoflagellates and prokaryotes show less temporal changes than diatoms.

[49] Subpolar latitudes exhibit the same type of variability as temperate latitudes (i.e., changes in timing and magnitude of the bloom; Figure 10). However, the mean annual pattern is more persistent and the range of variations in total and class-specific primary production is somewhat narrower. For example, anomalies range between −15% and +21% for
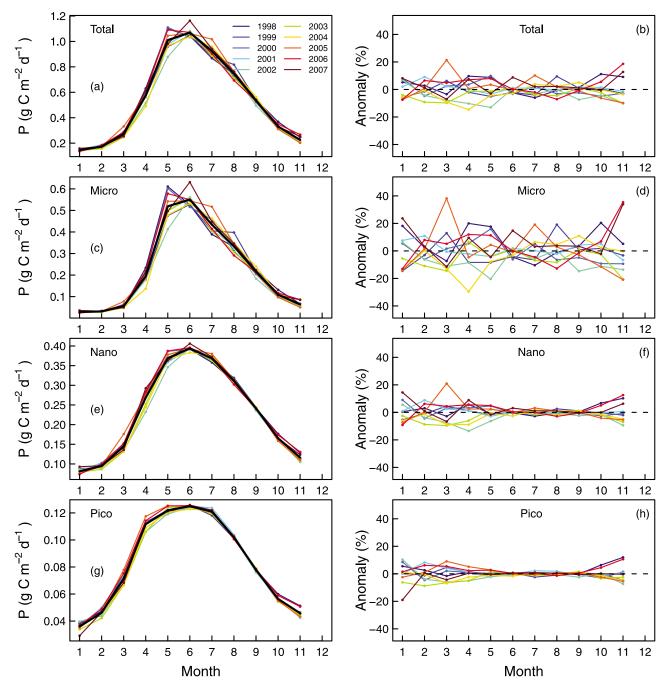
Figure 10. As Figure 7, but for the subpolar North Atlantic [50°N–70°N; 10°W–60°W].

P_{tot}, and −30% and +38% for P_{micro} (compared to −14% and +30% for P_{tot}, and −26% and +52% for P_{micro} at temperate latitudes).

[50] Several studies were dedicated to analyzing satellite Chl_{surf} data within the context of mechanisms responsible for the temporal variability in timing and magnitude of the North Atlantic bloom [e.g., *Follows and Dutkiewicz*, 2002; *Stramska*, 2005]. This variability results primarily from interannual changes in the physical forcing of the bloom, mainly winter mixing and preconditioning, and spring stratification onset [*Follows and Dutkiewicz*, 2002; *Waniek*,

2003; *Henson et al.*, 2006]. Depending on season and latitude, intermittent wind mixing events may favor (via nutrient supply) or inhibit (via light limitation) phytoplankton growth, thus perturbing the "usual" development of the bloom. Biotic factors, such as grazing, also come into play and control the intensity and termination of the bloom [*Siegel et al.*, 2002; *Henson et al.*, 2006].

3.2.4. Phytoplankton Class-Specific Variability

[51] Our analysis indicates that microphytoplankton are associated with the largest range of variability of the three phytoplankton classes, both on seasonal (Figures 2–5) and

interannual (Figures 7–10) time scales. The time and space variability of microphytoplankton (diatoms) production is largely explained by the opportunistic nature of diatoms, which are the most responsive to sporadic changes in abiotic factors (nutrient inputs; [*Fogg*, 1991]), and are also sensitive to biotic factors (grazing). Conversely, smaller cells are favored by more constant environmental conditions. This pattern applies over the full trophic range encountered in the open ocean. It is not only observed in temperate and subpolar latitude environments but also in more stable oligotrophic systems, where erosion of the nutricline and subsequent injection of nutrients to the euphotic zone occurs via vertical mixing [*Riser and Johnson*, 2008] or deepening of the euphotic depth [*Letelier et al.*, 2004]. On an interannual time scale, modifications in environmental conditions influence the composition of the phytoplankton community and associated primary production, especially diatom production. Because diatoms are recognized as the main drivers of new production and carbon export, such interannual changes are likely to have profound consequences in terms of biogeochemical carbon cycling. This points to the importance of resolving changes in phytoplankton community composition when interpreting time series of biomass or primary production.

4. Conclusions

[52] The present study utilizes the 10-year time series of SeaWiFS ocean color data to estimate total and phytoplankton class-specific primary production within the world's open oceans during the past decade. Our approach is unique in that it enables deriving depth-resolved fields of primary production associated with three major phytoplankton size classes or taxonomic groups. This approach accounts for the dependence of primary production on community composition, vertical distribution of Chl biomass, photophysiology, and irradiance within the water column. In that sense, it offers a compromise and an alternative to traditional Chl-based [e.g., *Longhurst et al.*, 1995; *Antoine et al.*, 1996; *Behrenfeld and Falkowski*, 1997b] and new carbon-based models [*Behrenfeld et al.*, 2005; *Westberry et al.*, 2008]. In addition, our approach can complement the surface data derived from algorithms for discriminating phytoplankton groups from space [*Alvain et al.*, 2005; *Hirata et al.*, 2008] by providing quantitative information within the entire upper water column (i.e., 0–$1.5Z_{eu}$).

[53] Assessing climatology and interannual changes in primary production associated with three major phytoplankton classes within the global ocean represents a significant contribution to our ability to understand and quantify carbon cycling in the upper ocean. For example, global estimates of phytoplankton class-specific primary production rates are key parameters required to parameterize and validate global biogeochemical models that explicitly incorporate diverse phytoplankton groups [*Le Quéré et al.*, 2005; *Hood et al.*, 2006]. These estimates also provide a benchmark for monitoring the response of pelagic ecosystems to climate change in terms of changes in biodiversity of phytoplankton communities and associated carbon fluxes.

This has important implications for understanding feedbacks between biogeochemical cycles and climate changes.

[54] One important question that deserves attention in future studies is a thorough analysis of year-to-year variations in class-specific primary production in relation to environmental changes. To pursue this task, the primary production time series would have to be examined simultaneously with changes in forcing factors such as light, mixed layer depth, temperature, or nutrient availability. This type of analyses cannot be done using conventional monthly climatology of oceanographic data. It would greatly benefit from a synergistic coupling with data collected by Argo-type autonomous bio-optical profiling floats. These floats allow simultaneous monitoring of physical and biological properties within the ocean interior over broad areas and long time periods [e.g., *Johnson et al.*, 2009]. As demonstrated in several studies, such data provide invaluable information to validate and complement surface satellite-derived biogeochemical products within the ocean interior and areas obscured by clouds [*Bishop et al.*, 2002; *Boss et al.*, 2008; *Riser and Johnson*, 2008].

References

Agawin, N. S. R., C. M. Duarte, and S. Agusti (2000), Nutrient and temperature control of the contribution of picoplankton to phytoplankton biomass and production, *Limnol. Oceanogr.*, *45*(3), 591–600.

Aiken, J., Y. Pradhan, R. Barlow, S. Lavender, A. J. Poulton, P. M. Holligan, and N. J. Hardman-Mountford (2009), Phytoplankton pigments and functional types in the Atlantic Ocean: A decadal assessment, 1995–2005, *Deep Sea Res., Part II*, *56*(15), 899–917, doi:10.1016/j.dsr2.2008.09.017.

Alvain, S., C. Moulin, Y. Dandonneau, and F. M. Bréon (2005), Remote sensing of phytoplankton groups in case I waters from global SeaWiFS imagery, *Deep Sea Res., Part I*, *52*(11), 1989–2004, doi:10.1016/j.dsr.2005.06.015.

Antoine, D., and A. Morel (1996), Oceanic primary production: 1. Adaptation of a spectral light-photosynthesis model in view of application to satellite chlorophyll observations, *Global Biogeochem. Cycles*, *10*(1), 43–55, doi:10.1029/95GB02831.

Antoine, D., J. M. André, and A. Morel (1996), Oceanic primary production 2. Estimation at global scale from satellite (coastal zone color scanner) chlorophyll, *Global Biogeochem. Cycles*, *10*(1), 57–69, doi:10.1029/95GB02832.

Aumont, O., E. Maier-Reimer, S. Blain, and P. Monfray (2003), An ecosystem model of the global ocean including Fe, Si, P colimitations, *Global Biogeochem. Cycles*, *17*(2), 1060, doi:10.1029/2001GB001745.

Barber, R. T., and F. P. Chavez (1991), Regulation of primary productivity rate in the equatorial Pacific, *Limnol. Oceanogr.*, *36*(8), 1803–1815, doi:10.4319/lo.1991.36.8.1803.

Behrenfeld, M. J., and P. G. Falkowski (1997a), A consumer's guide to phytoplankton primary productivity models, *Limnol. Oceanogr.*, *42*(7), 1479–1491, doi:10.4319/lo.1997.42.7.1479.

Behrenfeld, M. J., and P. G. Falkowski (1997b), Photosynthetic rates derived from satellite-based chlorophyll concentration, *Limnol. Oceanogr.*, *42*(1), 1–20, doi:10.4319/lo.1997.42.1.0001.

Behrenfeld, M. J., E. Boss, D. A. Siegel, and D. M. Shea (2005), Carbon-based ocean productivity and phytoplankton physiology from space, *Global Biogeochem. Cycles*, *19*, GB1006, doi:10.1029/2004GB002299

Behrenfeld, M. J., R. T. O'Malley, D. A. Siegel, C. R. McClain, J. L. Sarmiento, G. C. Feldman, A. J. Milligan, P. G. Falkowski, R. M. Letelier, and E. S. Boss (2006), Climate-driven trends in contemporary ocean productivity, *Nature*, *444*(7120), 752–755, doi:10.1038/nature05317.

Bidigare, R. R., B. B. Prézelin, and R. C. Smith (1992), Bio-optical models and the problems of scaling, in *Primary Productivity and Biogeochemical Cycles in the Sea*, edited by P. G. Falkowski and A. D. Woodhead, pp. 175–212, Plenum Press, New York.

Bishop, J. K. B., R. E. Davis, and J. T. Sherman (2002), Robotic observations of dust storm enhancement of carbon biomass in the North Pacific, *Science*, 298(5594), 817–821, doi:10.1126/science.1074961.

Blanchot, J., J. M. André, C. Navarette, J. Neveux, and M. H. Radenac (2001), Picophytoplankton in the equatorial Pacific: Vertical distributions in the warm pool and in the high nutrient low chlorophyll conditions, *Deep Sea Res., Part I*, 48(1), 297–314, doi:10.1016/S0967-0637(00)00063-7.

Bosc, E., A. Bricaud, and D. Antoine (2004), Seasonal and interannual variability in algal biomass and primary production in the Mediterranean Sea, as derived from 4 years of SeaWiFS observations, *Global Biogeochem. Cycles*, 18, GB1005, doi:10.1029/2003GB002034.

Boss, E., D. Swift, L. Taylor, P. Brickley, R. Zaneveld, S. Riser, M. J. Perry, and P. G. Strutton (2008), Observations of pigment and particle distributions in the western North Atlantic from an autonomous float and ocean color satellite, *Limnol. Oceanogr.*, 53(5), 2112–2122.

Bouman, H. A., T. Platt, S. Sathyendranath, and V. Stuart (2005), Dependence of light-saturated photosynthesis on temperature and community structure, *Deep Sea Res., Part I*, 52(7), 1284–1299, doi:10.1016/j.dsr.2005.01.008.

Boyd, P. W. (2002), Environmental factors controlling phytoplankton processes in the Southern Ocean, *J. Phycol.*, 38, 844–861, doi:10.1046/j.1529-8817.2002.t01-1-01203.x.

Bricaud, A., H. Claustre, J. Ras, and K. Oubelkheir (2004), Natural variability of phytoplankton absorption in oceanic waters: Influence of the size structure of algal populations, *J. Geophys. Res.*, 109, C11010, doi:10.1029/2004JC002419.

Bury, S. J., P. W. Boyd, T. Preston, G. Savidge, and N. J. P. Owens (2001), Size-fractionated primary production and nitrogen uptake during a North Atlantic phytoplankton bloom: Implications for carbon export estimates, *Deep Sea Res., Part I*, 48(3), 689–720, doi:10.1016/S0967-0637(00)00066-2.

Cailliau, C., H. Claustre, and S. Giannino (1997), Chemotaxonomic analysis of phytoplankton distribution in the Indian sector of the Southern Ocean during late austral Summer, *Oceanol. Acta*, 20(5), 721–732.

Cermeño, P., P. Estévez-Blanco, E. Marañon, and E. Fernandez (2005), Maximum photosynthetic efficiency of size-fractionated phytoplankton assessed by ^{14}C uptake and fast repetition rate fluorometry, *Limnol. Oceanogr.*, 50(5), 1438–1446.

Chavez, F. P., and R. T. Barber (1987), An estimate of new production in the equatorial Pacific, *Deep Sea Res., Part A*, 34(7), 1229–1243.

Chavez, F. P., K. R. Buck, and R. T. Barber (1990), Phytoplankton taxa in relation to primary production in the equatorial Pacific, *Deep Sea Res., Part A*, 37(11), 1733–1752.

Chavez, F. P., K. R. Buck, S. K. Service, J. Newton, and R. T. Barber (1996), Phytoplankton variability in the central and eastern tropical Pacific, *Deep Sea Res., Part II*, 43(4–6), 835–870, doi:10.1016/0967-0645(96)00028-8.

Chisholm, S. W. (1992), Phytoplankton size, in *Primary Productivity and Biogeochemical Cycles in the Sea*, edited by P. G. Falkowski and A. D. Woodhead, pp. 213–237, Plenum Press, New York.

Chisholm, S. W., and F. M. M. Morel (1991), What controls phytoplankton production in nutrient-rich areas of the open sea?, *Am. Soc. Limnol. Oceanogr. Symp.*, Preface, 36(8), U1507–U1511.

Ciotti, A. M., and A. Bricaud (2006), Retrievals of a size parameter for phytoplankton and spectral light absorption by colored detrital matter from water-leaving radiances at SeaWiFS channels in a continental shelf region off Brazil, *Limnol. Oceanogr. Methods*, 4, 237–253.

Claustre, H. (1994), The trophic status of various oceanic provinces as revealed by phytoplankton pigment signatures, *Limnol. Oceanogr.*, 39(5), 1206–1210, doi:10.4319/lo.1994.39.5.1206.

Claustre, H., and J. C. Marty (1995), Specific phytoplankton biomasses and their relation to primary production in the tropical North Atlantic, *Deep Sea Res., Part I*, 42(8), 1475–1493, doi:10.1016/0967-0637(95)00053-9.

Claustre, H., P. Kerherve, J. C. Marty, L. Prieur, C. Videau, and J. H. Hecq (1994), Phytoplankton dynamics associated with a geostrophic front: Ecological and biogeochemical implications, *J. Mar. Res.*, 52, 711–742, doi:10.1357/0022240943077000.

Claustre, H., M. A. Moline, and B. B. Prézelin (1997), Sources of variability in the column photosynthetic cross section for Antarctic coastal waters, *J. Geophys. Res.*, 102(C11), 25,047–25,060, doi:10.1029/96JC02439.

Claustre, H., M. Babin, D. Merien, J. Ras, L. Prieur, S. Dallot, O. Prasil, H. Dousova, and T. Moutin (2005), Towards a taxon-specific parameter-

ization of bio-optical models of primary production: A case study in the North Atlantic, *J. Geophys. Res.*, 110, C07S12, doi:10.1029/2004JC002634.

Coale, K. H., S. E. Fitzwater, R. M. Gordon, K. S. Johnson, and R. T. Barber (1996), Control of community growth and export production by upwelled iron in the equatorial Pacific Ocean, *Nature*, 379, 621–624, doi:10.1038/379621a0.

Dandonneau, Y., P. Y. Deschamps, J. M. Nicolas, H. Loisel, J. Blanchot, Y. Montel, F. Thieuleux, and G. Becu (2004), Seasonal and interannual variability of ocean color and composition of phytoplankton communities in the North Atlantic, equatorial Pacific and South Pacific, *Deep Sea Res., Part II*, 51(1–3), 303–318, doi:10.1016/j.dsr2.2003.07.018.

de Boyer Montégut, C., G. Madec, A. S. Fischer, A. Lazar, and D. Iudicone (2004), Mixed layer depth over the global ocean: An examination of profile data and a pofile-based climatology, *J. Geophys. Res.*, 109, C12003, doi:10.1029/2004JC002378.

Dickey, T., et al. (2001), Physical and biogeochemical variability from hours to years at the Bermuda Testbed Mooring site: June 1994-March 1998, *Deep Sea Res., Part II*, 48(8–9), 2105–2140, doi:10.1016/S0967-0645(00)00173-9.

Dugdale, R. C., and F. P. Wilkerson (1992), Nutrient limitation of new production in the sea, in *Primary Productivity and Biogeochemical Cycles in the Sea*, edited by P. G. Falkowski and A. D. Woodhead, pp. 107–122, Plenum Press, New York.

Dugdale, R. C., and F. P. Wilkerson (1998), Silicate regulation of new production in the equatorial Pacific upwelling, *Nature*, 391(6664), 270–273, doi:10.1038/34630.

Eppley, R. W., and B. J. Peterson (1979), Particulate organic matter flux and planktonic new production in the deep ocean, *Nature*, 282(5740), 677–680, doi:10.1038/282677a0.

Falkowski, P. G., and J. A. Raven (1997), Aquatic photosynthesis in biogeochemical cycles, in *Aquatic Photosynthesis*, edited by P. G. Falkowski and J. A. Raven, pp. 300–335, Blackwell Sci., Oxford, U. K.

Falkowski, P. G., R. M. Greene, and R. J. Geider (1992), Physiological limitations on phytoplankton productivity in the ocean, *Oceanography*, 5, 84–91.

Falkowski, P. G., M. Katz, A. H. Knoll, A. Quigg, J. A. Raven, O. M. Schofield, and F. J. R. Taylor (2004), The evolution of modern eukaryotic phytoplankton, *Science*, 305, 354–360, doi:10.1126/science.1095964.

Fiedler, P. C., V. Philbrick, and F. P. Chavez (1991), Oceanic upwelling and productivity in the eastern tropical Pacific, *Limnol. Oceanogr.*, 36(8), 1834–1850, doi:10.4319/lo.1991.36.8.1834.

Findlay, H. S., A. Yool, M. Nodale, and J. W. Pitchford (2006), Modelling of autumn plankton bloom dynamics, *J. Plankton Res.*, 28(2), 209–220, doi:10.1093/plankt/fbi114.

Fogg, G. E. (1991), The phytoplanktonic ways of life, *New Phytol.*, 118(2), 191–232, doi:10.1111/j.1469-8137.1991.tb00974.x.

Follows, M. J., and S. Dutkiewicz (2002), Meteorological modulation of the North Atlantic spring bloom, *Deep Sea Res., Part II*, 49(1–3), 321–344.

Goffart, A., G. Catalano, and J. H. Hecq (2000), Factors controlling the distribution of diatoms and Phaeocystis in the Ross Sea, *J. Mar. Syst.*, 27(1–3), 161–175, doi:10.1016/S0924-7963(00)00058-0.

Goldman, J. C. (1993), Potential role of large oceanic diatoms in new primary production, *Deep Sea Res., Part I*, 40, 159–168, doi:10.1016/0967-0637(93)90059-C.

Guidi, L., L. Stemmann, G. A. Jackson, F. Ibanez, H. Claustre, L. Legendre, M. Picheral, and G. Gorsky (2010), Effects of phytoplankton community on production, size, and export of large aggregates: A World-Ocean analysis, *Limnol. Oceanogr.*, 54(6), 1951–1963.

Harrison, P. J., P. W. Boyd, D. E. Varela, S. Takeda, A. Shiomoto, and T. Odate (1999), Comparison of factors controlling phytoplankton productivity in the NE and NW subarctic Pacific gyres, *Prog. Oceanogr.*, 43(2–4), 205–234, doi:10.1016/S0079-6611(99)00015-4.

Henson, S. A., I. Robinson, J. T. Allen, and J. J. Waniek (2006), Effect of meteorological conditions on interannual variability in timing and magnitude of the spring bloom in the Irminger Basin, North Atlantic, *Deep Sea Res., Part I*, 53(10), 1601–1615, doi:10.1016/j.dsr.2006.07.009.

Hirata, J. A., J. Aiken, N. J. Hardman-Mountford, T. J. Smyth, and R. Barlow (2008), An absorption model to derive phytoplankton size classes from satellite ocean color, *Remote Sens. Environ.*, 112, 3153–3159, doi:10.1016/j.rse.2008.03.011.

Hirata, T., N. J. Hardman-Mountford, R. Barlow, T. Lamont, R. Brewin, T. Smyth, and J. Aiken (2010), An inherent optical property approach to the estimation of size-specific photosynthetic rates in eastern boundary upwelling zones from satellite ocean colour: An initial assessment, *Prog. Oceanogr.*, 83(1–4), 393–397.

Holligan, P. M., et al. (1993), A biogeochemical study of the coccolithophore, Emiliania-Huxleyi, in the North-Atlantic, *Global Biogeochem. Cycles*, 7(4), 879–900, doi:10.1029/93GB01731.

Hood, R. R., et al. (2006), Pelagic functional group modeling: Progress, challenges and prospects, *Deep Sea Res., Part II*, 53(5–7), 459–512, doi:10.1016/j.dsr2.2006.01.025.

Iglesias-Rodriguez, M. D., C. W. Brown, S. C. Doney, J. A. Kleypas, D. D. Kolber, Z. S. Kolber, P. K. Hayes, and P. G. Falkowski (2002), Representing key phytoplankton functional groups in ocean carbon cycle models: Coccolithophorids, *Global Biogeochem. Cycles*, 16(4), 1100, doi:10.1029/2001GB001454.

Johnson, K. S., W. M. Berelson, E. S. Boss, Z. Chases, H. Claustre, S. R. Emerson, N. Gruber, A. Kortzinger, M. J. Perry, and S. C. Riser (2009), Observing biogeochemical cycles at global scales with profiling floats and gliders: Prospects for a global array, *Oceanography*, 22(3), 216–225.

Jordan, R. W., and A. H. L. Chamberlain (1997), Biodiversity among haptophyte algae, *Biodivers. Conserv.*, 6(1), 131–152, doi:10.1023/A:1018383817777.

Kameda, T., and J. Ishizaka (2005), Size-fractionated primary production estimated by a two-phytoplankton community model applicable to ocean color remote sensing, *J. Oceanogr.*, 61, 663–672, doi:10.1007/s10872-005-0074-7.

Kiørboe, T. (1993), Turbulence, phytoplankton cell size, and the structure of pelagic food webs, *Adv. Mar. Biol.*, 29(1), 1–72, doi:10.1016/S0065-2881(08)60129-7.

Koeve, W. (2001), Wintertime nutrients in the North Atlantic: New approaches and implications for new production estimates, *Mar. Chem.*, 74(4), 245–260, doi:10.1016/S0304-4203(01)00016-0.

Kudela, R. M., and R. C. Dugdale (2000), Nutrient regulation of phytoplankton productivity in Monterey Bay, California, *Deep Sea Res., Part II*, 47(5–6), 1023–1053, doi:10.1016/S0967-0645(99)00135-6.

Laws, E. A., P. G. Falkowski, W. O. Smith Jr., H. Ducklow, and J. J. McCarthy (2000), Temperature effects on export production in the open ocean, *Global Biogeochem. Cycles*, 14(4), 1231–1246, doi:10.1029/1999GB001229.

Le Quéré, C., et al. (2005), Ecosystem dynamics based on plankton functional types for global ocean biogeochemistry models, *Global Change Biol.*, 11(11), 2016–2040.

Letelier, R. M., D. M. Karl, M. R. Abbott, and R. R. Bidigare (2004), Light driven seasonal patterns of chlorophyll and nitrate in the lower euphotic zone of the North Pacific subtropical gyre, *Limnol. Oceanogr.*, 49(2), 508–519.

Li, W. K. W. (1994), Primary production of prochlorophytes, cyanobacteria, and eukaryotic ultraphytoplankton: Measurements from flow cytometric sorting, *Limnol. Oceanogr.*, 39(1), 169–175.

Liu, H., I. Probert, J. Uitz, H. Claustre, S. Aris-Brosou, M. Frada, F. Not, and C. de Vargas (2009), Extreme diversity in noncalcifying haptophytes explains a major pigment paradox in open oceans, *Proc. Natl. Acad. Sci. U. S. A.*, 106(31), 12,803–12,808, doi:10.1073/pnas.0905841106.

Lochte, K., H. W. Ducklow, M. J. R. Fasham, and C. Stienen (1993), Plankton succession and carbon cycling at 47°N 20°W during the JGOFS North-Atlantic Bloom Experiment, *Deep Sea Res., Part II*, 40(1–2), 91–114, doi:10.1016/0967-0645(93)90008-B.

Longhurst, A. R. (2007), *Ecological Geography of the Sea*, 2nd ed., Academic, San Diego, Calif.

Longhurst, A. R., S. Sathyendranath, T. Platt, and C. M. Caverhill (1995), An estimate of global primary production in the ocean from satellite radiometer data, *J. Plankton Res.*, 17(6), 1245–1271, doi:10.1093/plankt/17.6.1245.

Lutz, M. J., K. Caldeira, R. B. Dunbar, and M. J. Behrenfeld (2007), Seasonal rhythms of net primary production and particulate organic carbon flux to depth describe the efficiency of biological pump in the global ocean, *J. Geophys. Res.*, 112, C10011, doi:10.1029/2006JC003706.

Malone, T. C. (1980), Algal size, in *The Physiological Ecology of Phytoplankton*, edited by I. Morris, pp. 433–463, Univ. of Calif., Berkeley.

Marañon, E., P. M. Holligan, M. Varela, B. Mourino, and A. J. Bale (2000), Basin-scale variability of phytoplankton biomass, production and growth in the Atlantic Ocean, *Deep Sea Res., Part I*, 47(5), 825–857, doi:10.1016/S0967-0637(99)00087-4.

Margalef, R. (1965), Ecological correlation and relationship between primary producing and plankton structure, *Mem. Ist. Ital. Idrobiol.*, 18, 355–364.

Martin, J. H., R. M. Gordon, and S. E. Fitzwater (1991), The case for iron, *Limnol. Oceanogr.*, 36(8), 1793–1802, doi:10.4319/lo.1991.36.8.1793.

McClain, C. R. (2009), A decadal of satellite ocean color observations, *Annu. Rev. Mar. Sci.*, 1, 19–42, doi:10.1146/annurev.marine.010908.163650.

McPhaden, M. J. (1999), Genesis and evolution of the 1997–98 El Niño, *Science*, 283(5404), 950–954, doi:10.1126/science.283.5404.950.

Michaels, A. F., and M. W. Silver (1988), Primary production, sinking fluxes and the microbial food web, *Deep Sea Res.*, 35, 473–490, doi:10.1016/0198-0149(88)90126-4.

Miller, C. B., B. W. Frost, P. A. Wheeler, M. R. Landry, N. A. Welschmeyer, and T. M. Powell (1991), Ecological dynamics in the subarctic Pacific, a possibly iron-limited ecosystem, *Limnol. Oceanogr.*, 36(8), 1600–1615, doi:10.4319/lo.1991.36.8.1600.

Mitchell, B. G., E. A. Brody, O. Holm-Hansen, C. R. McClain, and J. K. B. Bishop (1991), Light limitation of phytoplankton biomass and macronutrient utilization in the Southern Ocean, *Limnol. Oceanogr.*, 36(8), 1662–1677, doi:10.4319/lo.1991.36.8.1662.

Moon van der Staay, S. Y., G. W. M. van der Staay, L. Guillou, D. Vaulot, H. Claustre, and L. K. Medlin (2000), Abundance and diversity of prymnesiophytes in the picoplankton community from the equatorial Pacific Ocean inferred from 18S rDNA sequences, *Limnol. Oceanogr.*, 45(1), 98–109, doi:10.4319/lo.2000.45.1.0098.

Moore, J. K., S. C. Doney, D. M. Glover, and I. Y. Fung (2002), Iron cycling and nutrient-limitation patterns in surface waters of the world ocean, *Deep Sea Res., Part II*, 49, 463–507, doi:10.1016/S0967-0645(01)00109-6.

Morel, A. (1991), Light and marine photosynthesis: A spectral model with geochemical and climatological implications, *Prog. Oceanogr.*, 26, 263–306, doi:10.1016/0079-6611(91)90004-6.

Morel, A., and J. F. Berthon (1989), Surface pigments, algal biomass profiles, and potential production of the euphotic layer: Relationships reinvestigated in view of remote-sensing applications, *Limnol. Oceanogr.*, 34(8), 1545–1562, doi:10.4319/lo.1989.34.8.1545.

Morel, A., and S. Maritorena (2001), Bio-optical properties of oceanic waters: A reappraisal, *J. Geophys. Res.*, 106(C4), 7163–7180, doi:10.1029/2000JC000319.

Morel, A., D. Antoine, M. Babin, and Y. Dandonneau (1996), Measured and modeled primary production in the northeast Atlantic (EUMELI JGOFS program): The impact of natural variations in photosynthetic parameters on model predictive skill, *Deep Sea Res., Part I*, 43(8), 1273–1304, doi:10.1016/0967-0637(96)00059-3.

Ondrusek, M. E., R. R. Bidigare, S. T. Sweet, D. A. Defreitas, and J. M. Brooks (1991), Distribution of phytoplankton pigments in the North Pacific Ocean in relation to physical and optical variability, *Deep Sea Res., Part I*, 38(2), 243–266, doi:10.1016/0198-0149(91)90082-Q.

Partensky, F., J. Blanchot, and D. Vaulot (1999), Differential distribution and ecology of Prochlorococcus and Synechococcus in oceanic waters: A review, *Bull. Inst. Océanogr.*, 457–475.

Pennington, J. T., K. L. Mahoney, V. S. Kuwahara, D. D. Kolber, R. Calienes, and F. P. Chavez (2006), Primary production in the eastern tropical Pacific: A review, *Prog. Oceanogr.*, 69(2–4), 285–317, doi:10.1016/j.pocean.2006.03.012.

Ras, J., H. Claustre, and J. Uitz (2008), Spatial variability of phytoplankton pigment distributions in the subtropical South Pacific Ocean: Comparison between in situ and modelled data, *Biogeosciences*, 5, 353–369, doi:10.5194/bg-5-353-2008.

Raven, J. A. (1998), Small is beautiful: The picophytoplankton, *Funct. Ecol.*, 12(4), 503–513, doi:10.1046/j.1365-2435.1998.00233.x.

Riser, S. C., and K. S. Johnson (2008), Net production of oxygen in the subtropical ocean, *Nature*, 451(7176), 323–325, doi:10.1038/nature06441.

Sathyendranath, S., L. Watts, E. Devred, T. Platt, C. M. Caverhill, and H. Maass (2004), Discrimination of diatom from other phytoplankton using ocean-colour data, *Mar. Ecol. Prog. Ser.*, 272, 59–68, doi:10.3354/meps272059.

Schoemann, V., S. Becquevort, J. Stefels, V. Rousseau, and C. Lancelot (2005), Phaeocystis blooms in the global ocean and their controlling mechanisms: A review, *J. Sea Res.*, 53, 43–66, doi:10.1016/j.seares.2004.01.008.

Siegel, D. A., S. C. Doney, and J. A. Yoder (2002), The North Atlantic spring phytoplankton bloom and Sverdrup's critical depth hypothesis, *Science*, 296(5568), 730–733, doi:10.1126/science.1069174.

Silió-Calzada, A., A. Bricaud, J. Uitz, and B. Gentili (2008), Estimation of new primary production in the Benguela upwelling area, using ENVISAT satellite data and a model dependant on the phytoplankton community size structure, *J. Geophys. Res.*, 113, C11023, doi:10.1029/2007JC004588.

Smetacek, V. (1999), Diatoms and the ocean carbon cycle, *Protist*, 150(1), 25–32, doi:10.1016/S1434-4610(99)70006-4.

Stramska, M. (2005), Interannual variability of seasonal phytoplankton blooms in the north polar Atlantic in response to atmospheric forcing, *J. Geophys. Res.*, 110, C05016, doi:10.1029/2004JC002457.

Strutton, P. G., and F. P. Chavez (2000), Primary productivity in the equatorial Pacific during the 1997–1998 El Niño, *J. Geophys. Res.*, *105*(C11), 26,089–26,101, doi:10.1029/1999JC000056.

Sverdrup, H. U. (1953), On conditions of the vernal blooming of phytoplankton, *J. Cons. Int. Explor. Mer*, *18*, 287–295.

Takahashi, T., et al. (2009), Climatological mean and decadal change in surface ocean pCO_2, and net sea-air CO_2 flux over the global oceans, *Deep Sea Res., Part II*, *56*(8–10), 554–577, doi:10.1016/j.dsr2.2008.12.009.

Tréguer, P., D. M. Nelson, A. J. Van Bennekom, D. J. DeMaster, A. Leynaert, and B. Quéguiner (1995), The silica balance in the world ocean: A reestimate, *Science*, *268*, 375–379, doi:10.1126/science.268.5209.375.

Tréguer, P., L. Legendre, R. T. Rivkin, O. Ragueneau, and N. Dittert (2003), Water column biogeochemistry below the euphotic zone, in *Ocean Biogeochemistry: The Role of Ocean Carbon Cycle in Global Change*, edited by M. J. R. Fasham, pp. 145–156, Springer, New York.

Uitz, J., H. Claustre, A. Morel, and S. B. Hooker (2006), Vertical distribution of phytoplankton communities in open ocean: An assessment based on surface chlorophyll, *J. Geophys. Res.*, *111*, C08005, doi:10.1029/2005JC003207.

Uitz, J., Y. Huot, F. Bruyant, M. Babin, and H. Claustre (2008), Relating phytoplankton photophysiological properties to community structure on large scale, *Limnol. Oceanogr.*, *53*(2), 614–630.

Uitz, J., H. Claustre, F. B. Griffiths, J. Ras, N. Garcia, and V. Sandroni (2009), A phytoplankton class-specific primary production model applied to the Kerguelen islands region (Southern Ocean), *Deep Sea Res., Part I*, *56*(4), 541–560, doi:10.1016/j.dsr.2008.11.006.

Vidussi, F., H. Claustre, B. B. Manca, A. Luchetta, and J. C. Marty (2001), Phytoplankton pigment distribution in relation to upper thermocline circulation in the eastern Mediterranean Sea during winter, *J. Geophys. Res.*, *106*(C9), 19,939–19,956, doi:10.1029/1999JC000308.

Waniek, J. J. (2003), The role of physical forcing in initiation of spring blooms in the northeast Atlantic, *J. Mar. Syst.*, *39*(1–2), 57–82, doi:10.1016/S0924-7963(02)00248-8.

Westberry, T., M. J. Behrenfeld, D. A. Siegel, and E. Boss (2008), Carbon-based primary productivity modeling with vertically resolved photoacclimation, *Global Biogeochem. Cycles*, *22*, GB2024, doi:10.1029/2007GB003078.

Yoder, J. A., and M. A. Kennelly (2003), Seasonal and ENSO variability in global ocean phytoplankton chlorophyll derived from 4 years of SeaWiFS measurements, *Global Biogeochem. Cycles*, *17*(4), 1112, doi:10.1029/2002GB001942.

Yoder, J. A., C. R. McClain, G. C. Feldman, and W. E. Esaias (1993), Annual cycles of phytoplankton chlorophyll concentrations in the global ocean: A satellite view, *Global Biogeochem. Cycles*, *7*(1), 181–193, doi:10.1029/93GB02358.

H. Claustre and B. Gentili, UMR 7093, LOV, UPMC Université Paris 6, CNRS, F-06238 Villefranche-sur-mer, France.

D. Stramski and J. Uitz, Marine Physical Laboratory, Scripps Institution of Oceanography, University of California, San Diego, La Jolla, California 92093-0238, USA. (juitz@ucsd.edu)